Title
A New Microfluidic Culture Platform to Manipulate Compressive Solid Stress on 3D Tissue

Author
Ford, Gretchen Hazel

Publication Date
2022

Peer reviewed|Thesis/dissertation

A New Microfluidic Culture Platform to Manipulate Compressive Solid Stress on 3D tissue

by
Gretchen Ford

DISSERTATION
Submitted in partial satisfaction of the requirements for degree of
DOCTOR OF PHILOSOPHY

in

Biophysics

in the

GRADUATE DIVISION
of the
UNIVERSITY OF CALIFORNIA, SAN FRANCISCO

Approved:

DocuSigned by:
Valerie Weaver
48C0A2F0F26A4A7...
Valerie Weaver
Chair

DocuSigned by:
Matthew Kutys
Matthew Kutys

DocuSigned by:
Tamara Alliston
Tamara Alliston

DocuSigned by:
Aaron Fields
Aaron Fields

DocuSigned by:
DAVID SCHAFFER
7462D9FCC764410...
DAVID SCHAFFER
Committee Members

To my parents, Grover and Madeliene Ford,

and my sister, Gabrielle Ford.

ACKNOWLEDGEMENTS

I am proud to present the body of work in this dissertation and to have earned my Ph.D., but it is not an accomplishment I could have achieved on my own. There are several individuals, both in and outside of the scientific community, whose support made this possible and to whom I am sincerely grateful. While it is challenging to properly express this gratitude in relatively few words, I will do my best.

First and foremost, I want to that I want to thank Professor Kristy Red-Horse at Stanford University. I applied to work in Professor Red-Horse's laboratory following the start of my graduate studies. At the time, Professor Red-Horse was on the path to achieving tenure, and although she interviewed more qualified candidates with previous research experience, she took a chance and hired me because I expressed great interest in a research career. I spent two years in Professor Red-Horse's lab, and it is almost certain that I would not have been admitted to this Ph.D. program without that experience. Moreover, Professor Red-Horse has continued to serve as a scientific mentor, and it has been truly a pleasure to keep in touch and meet up at scientific meetings over the course of my graduate studies.

Of course, I must thank both of my graduate advisors and mentors, Professor Valerie Weaver and Professor Matthew Kutys. First, Professor Weaver took a chance on me when I came to her as a "bright-eyed, bushy-tailed first-year graduate student" (her words) and asked to work in the Glioblastoma multiforme and solid stress space. Professor Weaver has been an excellent graduate advisor – she gave me the opportunity to explore many areas of interest, she challenged me to persevere through periods when progress felt slow, and she advocated for me in many professional arenas, ultimately helping me to find my path forward in science towards becoming a patent agent. When I reflect on my professional growth over the course of my

graduate studies, it is astounding how far I have come, and it is clear that Professors Weaver and Kutys facilitated much of that growth.

I must also thank Professor Matthew Kutys, at the start of my second year of graduate studies I became increasingly interested in incorporating an engineer's approach to uniquely study the impact of compressive stress in 3D tissues. Professor Kutys took me under his wing alongside Professor Weaver, taught me, challenged me, and enabled me to mold into the engineer and cell biologist I am today. For this I am forever grateful.

I also owe a great deal of thanks to all the members of the Weaver Lab I was fortunate enough to work with over the past few years. In particular, a huge thank you to Dr. Johnathon Lakins, who not only developed and optimized many of the key tools and methodologies that made my work possible, but also served as a day-to-day mentor and helped me think through and crystalize many of the key ideas and hypotheses that drove this work. Thanks also to Dr. Roger Oria Fernandez, who is a post doc in the Weaver Lab when I was tasked with learning physics-based simulation studies, Dr. Oria Fernandez was my go-to person for the endless stream of questions I had about designing experiments, if not for his patience and generosity with his time, I might have really struggled through my last couple of years in the lab. I'd also like to thank both Connor Stashko and Nadia Ayad, graduate students in the Weaver Lab for offering me their time to help me think through the many challenges I was tasked in my graduate work, if not for them I'd likely struggled in my final stages of my graduate studies. Finally, I'd like to thank all the members of the Kutys Lab, although we were a small group, we'd often provide guidance to one another as we faced challenges in our day- to- day experiments, and it was those interactions that challenged me to be a better scientist.

I would like to thank the Graduate Program in Bioengineering at UC Berkeley and UCSF forgiving me the opportunity to pursue a Ph.D. in such an exceptional environment. In particular, I would like to thank my other dissertation committee members, Professors Tamara Alliston, Aaron Fields, David Schaffer, and Matthew Kutys. Their critical and constructive feedback was

instrumental in guiding this work along the way, and each of them served as a mentor to me in a capacity well beyond their responsibility as a committee member. I am also grateful to the UCSF NIH T32 integrated Program in Complex Biological Systems Fellowship, not only for financially supporting me, but also because receiving the award was a major source of affirmation and motivation after numerous rejection letters from other fellowships.

A special thank you to Pierre Boivin, the best partner I could ask for. Its impossible to imagine how I would have accomplished this without his undying care and support through my graduate studies. Being a scientist himself, he has served as a mentor to me both professionally and personally as I faced the several challenges throughout the completion of this work. I'd also like to thank my in- laws for motivating me through my studies and being there to celebrate all the milestones along the way to the completion of this work.

Finally, thank you to my father, mother, and sister, for whom I've dedicated this dissertation. I have been so fortunate to belong to such a loving, caring, and supportive family. They have been behind me for every pursuit and challenge I have taken on, and there is no way I could have accomplished this without them. I know it was difficult for them, as it was for me, when I moved away from home to pursue this degree. I hope I can make them happy and proud by always continuing to strive for success in their honor.

ABSTRACT

A new microfluidic culture platform to manipulate compressive solid stress on 3D tissue

by

Gretchen H Ford

Compressive solid stress correlates with changes in the mechanical properties of developing confined tumors in the context of their microenvironment. Despite several advances to assay compressive solid stresses on cell and tissue behavior, the precise manipulation of compression in a 3D context remains challenging. Here, I introduce the design, generation and validation of a tractable microfluidic system that is able to isolate and manipulate compressive solid stresses in a controlled manner. Utilizing finite element analysis (FEA) I identify specific design parameters that permits application of 30% compression (strain) within my newly designed system. Importantly, particle image velocimetry (PIV) approaches enabled the measurement of strain via bead displacements which revealed that my microfluidic device demonstrates displacements that experimentally validated displacements predicted by FEA. Moreover, since PDMS is gas permeable a pressure sustainability assay was performed and resulted in a mean displacement of ~14μm in 14 hours, allowing for calculations of the appropriate amount of air to re-inject into my device to sustain 30% compression. Finally, I was able to demonstrate that 30% compression induces increases in area of patient- derived GBM neurospheres, and furthermore that this compressive solid stress- dependent size increase is functionally linked to integrin signaling through the focal adhesion kinase (pFAK) phosphorylation. I conclude that this novel tractable microdevice that I designed and validated can support the execution of controlled mechanistic studies aimed at elucidating the role of compressive solid stresses in 3D tissues. Accordingly, application of this device has strong potential to lead to new discoveries and therapies.

TABLE OF CONTENTS

LIST OF FIGURES

LIST OF TABLES

LIST OF ABBREVIATIONS

AFM atomic force microscopy

ECM extracellular matrix

EC endothelial cell

FN1 fibronectin 1

FAK focal adhesion kinase

FEA finite element analysis

GBM Glioblastoma muliforme

HA hyaluronic acid

MEC mammary epithelial cell

PDMS polydimethylsiloxane

RTK receptor tyrosine kinase

CHAPTER 1

Introduction

SOLID STRESS

Cells within tissues experience various physical stresses (force per unit area, N/m2, where N is Newtons and m is meters) at the meso- and micro- scale. These stresses include tensile solid stress, compressive solid stress, and shear stress. In brief, tensile (pull) and compressive (push) stresses are elicited when forces act perpendicular to the area of the object. Shear stress can be defined as two forces that act parallel to the area of the object. Tensile, compressive, and shear stresses are sensed at the tissue, cellular, and subcellar level (Figure 1.1).

At the tissue-level, tensile solid stress is experienced in response to bladder filling in urothelial cells (Merrill et al., 2016), compressive solid stress is subjected onto osteocytes in bone during weight bearing (Qin et al., 2020), and fluid/shear stress is experienced by endothelial cells in the lining of blood vessels during blood flow (Kutys and Chen, 2016). Additionally, cyclic shear solid stress is experienced by alveolar epithelial cells during oxygen intake in humans (Yang et al., 2020). Examples of forces at the cellular- level include those experienced within the inner ear canal in cochlear hair fiber cells through activation of ion channels induced by sound pressure waves (Goutman et al., 2015), in luminal epithelial cells within mammary ducts via adjacent highly contractile myoepithelial cells experience compressive solid stress (Adriance et al.,2005), and during cell- cell contact where neighboring cells exert forces against each other as expanding masses displace surrounding extracellular matrix (ECM) and healthy nearby tissue (Bazellieres et al.,2015). In the next section we discuss how forces are perceived at the subcellular level.

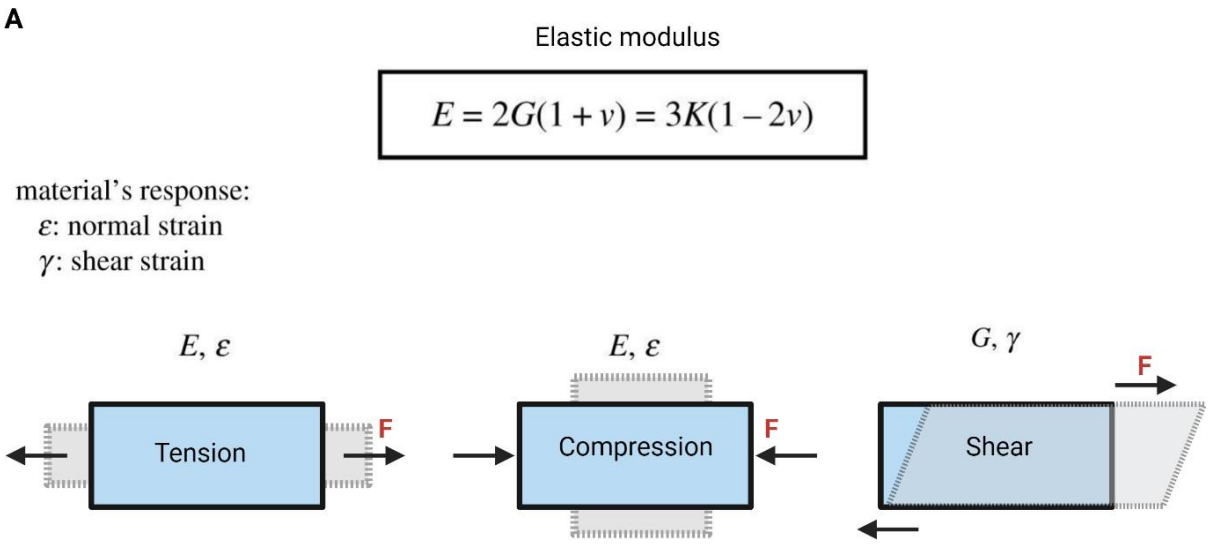

Figure 1.1: An overview of mechanical properties deforming under stress.
Schematic illustrating material resistance to elastic deformation to force (*F*) or stress (*σ*) is the elastic modulus. *E* is Young's modulus, a response to tensile or compressive stress, *G* is the shear modulus, a response to shear stress, and *K* is the bulk modulus, a response to hydrostatic pressure. The collection of these stresses such as tensile, compressive, and shear stresses occur at the tissue, cellular, and subcellular level.

HOW FORCES ARE PRECIEVED

Forces are perceived at the cellular and subcellular level through modifications in plasma membrane organization, ion channel activity, transmembrane receptor structure function and induction of actin cytoskeletal organization and actomyosin activation. For instance, caveolae are mechanoreceptors of high solid stresses (Lo et al., 2015; Cheng et al., 2015), disassembling in response to mechanical tension (hypo-osmotic shock or stretching), in an actin- and ATP-independent cell response (Sinha et al., 2011), shown in the embryonic notochord (Nixon et al., 2007), a precursor to the neural plate. Likewise, work from the Weaver laboratory demonstrated that, independent of actomyosin contractility, a bulky glycocalyx mediates tension by promoting integrin clustering (Paszek et al., 2014), indicating a novel mechanosensing role for this carbohydrate-rich structure. The size of the glycocalyx was measured with SAIM, a technique that permits high-resolution visualization of membrane structure. Other mechanotransduction roles for

glycocalyx include its response to blood flow in ECs, where it increases the production of nitric oxide by activating transient receptor potential channels in response to stretch (Dragovich et al., 2016). Through these mechanisms the cell is able to transform mechanical inputs such as tensile, compressive, and shear stresses into biochemical signals via unique molecular signaling responses that yield modified transcriptional outputs. Further, at the cellular level, cells within tissues sense material properties of neighboring cells and viscoelastic properties within the ECM through protein receptors and respond to these physical properties by generating tension and undergoing cytoskeletal reorganization through actomyosin in a dependent manner.

Force is crucial for tissue-specific development. For instance, mechanical stresses that are associated with blood flow—both cyclic strain and fluid shear stress are essential stimuli that function to form the vascular tree and promote heart chamber maturation during development (Kutys and Chen, 2016). Likewise, the fluid-filled luminal pressure in alveoli promotes branching morphogenesis during lung development (Nelson et al., 2017). Not surprisingly, developmental abnormalities that result in increased or decreased fluid pressure in the luminal cavity has potential to impair lung development, resulting in hyperplastic or hypoplastic lung branching, respectively (Blewett et al., 1996; Harding et al., 1993). These findings support a role for mechanical stress in directing tissue-specific development.

Disruption of tensional homeostasis is associated with a broad range of pathological conditions, this includes neurological deficiencies, inflammatory diseases, and tumorigenesis. Tumors are characterized by a stiffening of the stroma and an increase in the activity of mechanical receptors such as integrins and focal adhesion kinase, as has been reported for breast and pancreatic cancer (~4 kPa), which demonstrate increased activity of integrin focal adhesion signaling as indicated by phosphorylated focal adhesion kinase. These findings implicate tissue tension in malignancy. In fact, pathologic conditions of chronically increased stiffness such as cystic fibrosis and cirrhosis of the liver, which typically present with ECM accumulation, correlate with an increased risk of malignancy (Neglia et al., 1995; Bataller and

Brenner, 2005). Consistently, increased stromal stiffness has been linked to elevated lifetime risk for developing breast cancer (Paszek MJ, et al., 2005; Northey et al., JCI 2021) as well as breast and glioblastoma aggression (Miroshnikova, et al., 2016; Barnes et al., NCB 2018). Perturbed tissue forces are not only associated with cancer but also contribute to developmental abnormalities as has been reported for neural tube deficiencies.

MECHANOSENSING

Cells sense and transduce mechanical cues from the surrounding microenvironment through a process termed mechanotransduction. Specialized structures at both the membrane and intracellular level enable cells to sense force. Protein-based or cytoskeletal-and membrane mechanosensory structures mediate molecular responses to external forces. Further, cells are capable of sensing mechanical cues in various ways. This includes protein- based structures at the cell membrane known as ion channels. For example, in response to mechanical stimuli, ion channels Piezo1and Piezo2 that adopt an open confirmation under stretched conditions (Douguet and Honore´, 2019). Other mehcanosensing structures include integrins within focal adhesions (Kechagia et al., 2019) and cadherins in adherens junctions (Angulo-Urarte et al., 2020), as well as receptors cell- surface that facilitate cell-ECM and cell-cell interfaces. The collection of these interactions is linked to the actin cytoskeleton, facilitating the communication of mechanical cues both extrinsically and intrinsically to the cell. At the exterior region of the cell, forces can influence the ECM microenviornment to indirectly modulate cellular mechanotransduction. For instance, the organization of fibronectin (FN) which is a widely expressed ECM molecule can be dramatically modified in response to externally applied force. For example, fibronectin (FN) III domains can lengthen under 80–200 pN of force (Oberhauser et al., 2002,1998). The region within FN that is force unfolded thereafter permits cryptic binding sites within the FN III domain to become exposed due to mechanical stress (Sechler et al.,2001). Ligation of this additional FN binding site enhances $\alpha 5\beta 1$ integrin activity to foster focal adhesion assembly and facilitate fibronectin fibrillogenesis.

Similarly, fibrinogen can also be unfolded when met with forces of ~100 pN (Brown et al., 2007). This unfolding phenomenon can then stimulate its integrin receptor, macrophage-1 antigen(MAC1), which has been implicated in activation of inflammatory pathways (Deng et al., 2011). Further, mechanosensory structures on the cell surface change their confirmation in response to these extracellular stresses and modifications to ECM rigidity. Specifically, integrins are known for their confirmational changes. As the ECM stiffens integrins transform from a folded state to a stretched state, further enabling ligand binding (Case and Waterman, 2015) . ECM-integrin adhesions can acquire an increased lifespan followed by mechanical load. For example, under tensile stress, αbIIβ3 is associated with slip-bond behavior where the shelf-life of the bond is decreased. This behavior occurs at forces of 50–100 pN (Litvinovet al., 2011); other integrins such as α5β1 exposed to forces of 10–30pN reveals catch-bond behavior where the bond lifespan is increased (Kong et al., 2009; Roca-Cusachs et al., 2009). By these mechanisms, mechanosensory structures can adopt force- induced confirmational changes to shift to a mechanically adhesive or mechanosignaling function.

Physical cues are translated into biochemical signals by cells through various adaptor proteins and second messengers. In particular, integrins will bind to a compliant matrix (soft ECM) that leads to the establishment of short-lived focal points where the intracellular domain of the integrin is loosely bound to the actin cytoskeleton. However, when the same integrin is confronted with a stiff substrate ECM (stiff ECM) integrin clustering is fostered that triggers the recruitment of focal adhesion molecules to stimulate signaling pathways, where cells then undergo cytoskeletal remodeling to accommodate for reciprocal intracellular tension.

Growth and reinforcement of mechanosensitive focal adhesion structures occur through unfolding processes of proteins within integrin adhesions. For instance, 12 pN of force induces the unfolding of talin to uncover key binding sites which causes vinculin binding (del Rioetal.,2009), where, upon binding to talin, triggers the recruitment of intracellular plaque proteins at cytoplasmic tails of β- integrins ultimately potentiating the assembly of focal adhesions

(Bays and DeMali, 2017). Other force- induced conformational changes have been recorded in other focal adhesion associated proteins. For example, p130Cas is known to extend when subjected to mechanical stress. The extension of this protein leaves binding domains accessible for phosphorylation by SRC family kinases (Sa-wada et al., 2006). Thus, the regulation of downstream molecular signaling pathways is mediated by various mechanisms to ultimately elicit biological response and behaviors to mechanical stimuli.

MECHANOSIGNALING

Mechanosignals are translated at the cellular level into either transient or prolonged behavior. One example is cell response to ECM stiffness. In brief, cell proliferation and survival of the lung, as well as mammary epithelial cells (MEC) (Paszek et al., 2005), is activated via receptor tyrosine kinase (RTK) signaling to GTPase RAS which in turn stimulates MAPKs including ERK (Chess et al., 2000). Alternatively, force- dependent integrin signaling promotes dynamic responses that yield modified cell behaviors. For example, at the cellular level, activation of ERK enables its association with additional kinases, SRC and focal adhesion kinase(FAK), resulting in cell proliferation and sustained survival (Chaturvediet al., 2007). This has also been demonstrated for MAPK-dependent growth of keratinocytes upon subjection to mechanical stretch (Kippenberger et al.,2000), including osteocytes under load- bearing conditions (Plotkinet al., 2005).

Sustained cell responses to mechanical stress are developed through modifications in gene expression. For instance, elevated tensile stress can drive fibroblasts into a myofibroblast cell state, leading to remodeling and stiffening of the surrounding ECM (Piersma et al., 2020). Increased ECM proteins generate positive feedback (mechano- reciprocity) mechanism of which cells and tissues responding to mechanical stimuli begin to modify the structure, organization, and elasticity of the surrounding microenvironment.

QUANTIFYING SOLID STRESSES

Physical force (or stresses) can be directly quantified as a resulting strain or deformation within a region of interest. Mechanical properties are revealed through the study of the relationship between stress and strain. Young's modulus (E) is a unit that describes a purely elastic material under uniaxial deformation (compressive or tensile). In this context of elastic materials, other physical properties can be described as well. Materials that undergo shear stress, a physical force that is applied in the same plane as the cross- sectional area, has a measured property termed shear modulus (G).

Elastic materials deform and can return to its original form once stress is removed (Ayad et al., 2019). This feature is a consequence of the materials ability to store energy. These materials can undergo plastic deformation, a region where a material undergoes permanent deformation; where elastic regions end, and plastic begins. Elastic materials and their associated behavior are attractive as n they provide as a system that can withstand pressure and resist fracture. For example, polydimethylsiloxane (PDMS), although a viscoelastic material, is unique as it can be modified with crosslinking reagents to behave as a highly resilient elastic material (Natural and Synthetic Biomedical Polymers. Chapter 4, 2014). PDMS is especially important and favorably utilized in engineered microdevice technologies due to its linear siloxane backbone that has high flexibility, thermal stability, and is biocompatible.

Bulk modulus (K) is another elastic parameter and is related to hydrostatic pressure and is commonly utilized to quantify fluid flow. Poisson's ratio (v), which is a measurement of orthogonal deformation to an applied uniaxial stress, where: $2G\ (1 + v) = E = 3K\ (1 - 2\ v)$, relates material moduli to one another in isotropic materials. Moreover, the Poisson's ratio measures the deformation of a material in a direction perpendicular to the direction of the applied force. As materials are subjected to compressive or tensile stress the Poisson's effect illustrates expansion along one axis and contraction in the opposite axis (Greaves et al., 2011). The

Poisson's ratio is unitless and positive due to most common materials sharing narrowing within the cross- sectional regions. Majority of biomaterials acquire a Poisson's ratio between 0 and 0.5 where highly elastic materials illustrate a ratio near 0.5, meaning respective lateral stretching and expansion upon loading can occur. Poisson's ratio's closer to zero present minimal lateral stretch.

Compression is a force that is uniaxially applied toward the surface along the longitudinal axis resulting in a negative value for strain. Negative strain values stem from the shortening of an object along the direction of applied compression.

Tension is the uniaxial longitudinal lateral stretching of an object away from its surface that results in positive strain values [2] .To calculate the change in length we can use the following equation: $\Delta L = \frac{1}{E(elastic\ modulus)} \cdot \frac{F\ (force)}{A\ (area)} \cdot L_{0\ (original\ length)}$. The resulting value is used to describe the degree of strain formed from deformations caused by an applied force. Elastic modulus is the physical property that describes the materials resistance to elastic deformation to force [F] or stress [σ]. The term Young's modulus [E] is used to define responses to compressive and tensile stress and is commonly associated with the units of Pascals (Pa) (Ayad et al., 2019).

MATERIAL PROPERTIES

Viscoelastic materials acquire both an elastic and viscous component. The elastic portion of a viscoelastic material can store energy whereas its viscous counterparts dissipate energy (Chaudhuri et., 2020). Mechanical behavior of this material is time dependent. This involves how long an object is being deformed, the frequency of force applications, and the rate of amount of deformation. Viscoelastic materials have combinations of both covalent and non- covalent bonds. Non- covalent bonds are weak and arise upon energy dissipation from loading (Chaudhuri et., 2020; Ayad et al., 2019). These weak non- covalent bonds can break if the energy dissipation is on the same order as the time scale. Upon deformation, dissipation of energy, or loss in modulus, is lost in the form of heat due to friction from the breaking of non-covalent bonds that yield the entanglement and sliding of polymer chains within the material. In addition, these materials

display stress- relaxation when subjected to continuous deformation and increased strain. Creep, slow or permanent deformation under prolonged stress, is a potential feature if this material is under constant stress. Notably, viscoelastic materials failing to configure to its original form is owed to these characteristics. Specifically, these materials offer opportunity for modification independently of the initial elastic modulus, defines the slope of the stress-strain curve in the region of deformation, by increasing molecular weight. These options are favorable as it allows for increase in the ratio of covalent to non- covalent bonds and vary the loss modulus. Increasing covalent bonds through chemical modifications can decrease both loss modulus and energy dissipation.

Viscous materials have a stress that is dependent on the rate of deformation (not magnitude). This feature is due to dissipating energy from frictional interactions generated among adjacent layers of the fluid within the material (Chaudhuri et., 2020; Ayad et al., 2019). Since energy dissipation is consequential to shearing, when forces are being applied along the same plane or surface, between layers of fluid viscosity is often discussed in terms of shear forces. Linearly viscous materials have properties in which shear stress is proportional to shear rate.

Linear elastic materials, like elastic material, store energy and can undergo reversible deformation where the loading and unloading follow the same path (Chaudhuri et., 2020). For these materials stress is linearly proportional to strain. Non- linear elastic materials undergo irreversible deformations and do not have linear stress – strain relationships. For example, hyaluronic acid is viscoelastic non-linear material that exhibits biodegradability and biocompatibility. This hyaluronic acid hydrogel has a chemical structure that consists of a linear polysaccharide of d- glucuronic acid and N- acetyl – d- glucosamine (Kwon, et al., 2019). Since the viscous component of viscoelastic materials is subject to dissipative energy under deformation crosslinking methods can be used to decrease loss modulus and decrease dissipative energy (Chaudhuri et., 2020). Covalent bonds can be generated in the hyaluronic acid hydrogel by crosslinking methacrylate anhydride to hydroxyl groups on the hyaluronic polysaccharide

backbone resulting in an esterification reaction (Kwon, et al., 2019). This modification yields increased ratio of covalent to non-covalent weak bonds and decreases both loss modulus and dissipative energy which could allow for longer time scales of applied deformation. Altogether, when measuring material properties, variables E and G correspond to the elastic moduli and are proportional (not equal) to the stiffness of materials; though, majority of the biological literature uses E, G, elastic modulus and stiffness interchangeably.

METHODS TO PROBE CELL AND TISSUE SOLID STRESSES

At the tissue level, in vitro measurements involve utilization of compression- based assays (Galford et al., 1970) or indentation (Budday et al., 2019). These techniques require snap- frozen samples or the measurements of fresh hydrated post- mortem samples. Dynamic frequency sweep protocols, either in shear or tensile/compression mode has revealed viscous components of the brain, all of which is dependent on strain rate measurements (Chatelin et al., 2020).

The shear modulus is measured through the application of magnetic resonance elastography (MRE), which uses acoustic-range waves in a non-invasive manner to the tissue (Kruse et al., 2008; Sack et al., 2008). This method uses the high-frequency range, and as a result of brain viscoelasticity, the shear modulus measured via MRE is observed in the light of the frequency parameter when compared with traditional indentation and rheology techniques in the low-frequency range (Chatelin et al., 2010).

Measuring material properties of biological tissues can vary depending on specific modes used on the shear rheometer. For instance, it was discovered that glioma tissue is not stiffer than the brain at low shear strains when measured in a shear rheometer in the extension mode; but, when compression mode is employed, the glioma tissue was stiffer, increasing *G′* linearly with strain (Pogoda et al., 2014). This result suggests that there is a mechanism of compression stiffening in the brain microenvironment, where the collection of elevated vascularization and interstitial pressure can compress the brain impacting the mechanical properties of the tissue, as

opposed to increases in stromal rigidity due to the non-fibrous nature of the brain ECM. To that end, there is complex rheological behavior that occurs in brain tissue that requires close examination when comparing results concerning different complex modulus protocols, such as shear and compression mode.

Atomic force microscopy (AFM) is often used to achieve high resolution tissue and cellular measurements. This technique utilizes the measurement of the deflected cantilever after application of a defined forced and deformed sample. A probe that has a conical or spherical tip attached to the cantilever is typically used for indentation (Guz et al., 2014; Rico et al., 2005). Sharp tips are preferred for high- resolution imaging (Guz et al., 2014). To quantify the rigidity of cells via AFM, the Hertz model is used, as well as its assumptions (Dintwa et al., 2008). This is due to the model considering the cell as a linear elastic material within small deformations (<10% of the sample height). By contrast, various reports suggest that cells and the cytoskeleton are viscoelastic entities (Lu et al., 2006; Lee et al., 2018), and consequently depend on the deformation rate, including regions of small deformations. One report demonstrated that true elastic responses using AFM is observed especially when employing an optical trap while indenting upwards of 200 nm with 30 pN force (Nawaz et al., 2012).

While methods to investigate and assay the mechanical properties of the cell and tissue have been discussed, it's important to remember that cells naturally exert forces on their surroundings, and can result in compressive, tensile, or shear forces being transmitted into a biological response.

SOLID STRESSES ARE EXPERIENCED AT THE CELL AND TISSUE LEVEL

It is appreciated that endothelial cells (ECs), cells that line blood vessels, are subjected to hemodynamic shear stress as blood flows through the vessels. This is influenced by both the fluid viscosity and fluid flow velocities (Wirtz et al., 2011). Direct effects of this stress have been linked to cell cycle arrest (Lin et al., 2000), and accelerated EC turnover (Chiu et al., 1998). ECs also adopt an aligned and elongated phenotype that mimics the direction of flow under the appropriate

magnitudes and duration of flow. Moreover, under these conditions ECs have revealed a polygonal- like appearance with no clear orientation (Nigro et al., 2011). Metastatic processes subject the cells within a tumor to an array of further microenvironmental forces. As cells begin to migrate from the initial tumor site and transit into circulation, they become exposed to various solid and fluid stresses, most of which stimulate shear stress. Solid stresses can also elicit shear stress as ECs encounter tumor cells during intravasation and extravasation of the vasculature (Northcott et al., 2018). The physiological basal levels of shear stress [~5–30 dynes/cm^2(0.5–3 Pa)] inhibit mitosis and promote migration and adhesion of tumor cells (Avvisato et al., 2007; Mitchell and King, 2013; Ma et al., 2017; Xiong et al., 2017), while levels of shear stress like exercise conditions [60 dynes/cm^2(6 Pa)] potentiated tumor apoptosis (Regmi et al., 2017).

Solid stress (compressive and tensile) can be defined as forces exerted by the developing tumor and the resistance to deformation of the adjacent stromal tissue (Jain et al., 2014). Forces and strains that are transmitted away from the solid tumor mass to the neighboring stromal tissue, can yield remodeling and elevated ECM tension, including the interruption of the structure of the tumor (Jain et al., 2014). High ECM tension in these neighboring tissues might worsen by overcrowding from tumor-associated myofibroblast proliferation and immune cell permeation/growth throughout the desmoplastic and pro-inflammatory stromal responses. Moreover, variation in the material properties of the ECM (i.e., stiffening via deposition/remodeling) can also influence further growth and solid stress of the tumor. Hyaluronan can serve as a trap for interstitial fluids and swell upon hydration, ultimately resisting compression and elevated intratumoral solid stress (Jain et al., 2014). By contrast, collagen fibers acquire increased rigidity under tension resulting in resistance to further stretching (Jain et al., 2014). Prior to further tumor growth, the surrounding healthy tissue must be degraded or displaced. Simulation based studies have demonstrated that rigidity associated with a tumor must exceed 1.5 times that of the adjacent tissue for continued expansion (Voutouri et al., 2014). In opposition, an externally employed force can result in compressive stress or confinement of a tumor mass can result in

reduced cell division, stimulation of apoptosis/necrosis, enhanced ECM deposition/organization, and potentiate the invasive and metastatic ability of tumor cells (Yu et al., 2011). In fact, the external application of compression is necessary to decrease the volume and proliferative rate of cells within the core of spheroids grown in a 3D matrix (Helmlinger et al., 1997; Delarue et al., 2014; Mascheroni et al., 2016). Cell populations that proliferate at lower rates facilitate resistance to treatments and to the compressive stress of the tumor cells themselves may compromise the efficacy of chemotherapeutic agents (Mascheroni et al., 2017). In vivo, it has been demonstrated that one month of compression (at levels equivalent to those assessed in developing tumors), yields translocation of β-catenin from adherens junctions to the nucleus, stimulation of target genes for β-catenin, and enhanced colon crypt sizes (due to hyperplasia) (Fernández-Sánchez et al., 2015), suggesting that compressive stress can induce tumor growth. Solid stresses residing at the tumor periphery are sufficient to result in the compression of surrounding blood vessels, which leads to deformed elliptical shapes (Stylianopoulos et al., 2013). Obstruction and constriction of vasculature associated with the lymphatic system within the adjacent stroma results in decreased extravasated fluid (Jain et al., 2014). Therefore, the collection of solid stresses could induce increased interstitial fluid pressure (IFP) due to reduction within the interstitial area and the compromised collective fluid owing to obstructed vessels.

Glioblastoma multiforme (GBM), a tumor that grows in confinement, exerts stresses that could be exaggerated by the confinement of the brain by the skull. Altogether, a decrease in blood flow and enhanced IFP could result in both inadequate delivery of drugs of chemotherapeutics to the tumor and hypoxia (Zhang et al., 2014), which in turn lessens the effectiveness of radiation treatment (Mpekris et al., 2015).

TECHNOLOGIES TO STUDY SOLID STRESSES

Several state-of-the- art methods exist to date to assay biological behavior of cells and tissue under shear, tensile and compressive stress. One method of interrogating shear stress involves

a cone and plate device which was originally invented as a rheometer (Bowden et al., 2016). This works by rotating a cone- shaped insert apparatus atop a static plate to create a constant shear rate onto cells grown on the plate (Buschmann et al., 2005; Davies et al., 1984). This device can produce constant and homogenous flow patterns and is thus suitable for application of shear stress (Nagel et al., 1994). This cone-and-plate shearing method has been utilized to assay the effect of shear stress on inflammation, proliferation, apoptosis, and signaling pathways in ECs as well as vascular smooth muscle cells (Dai G et al., 2004; Gudi S et al., 1998; Ueba et al., 1997; Wagner et al., 1997; Yin et al., 2011). Another technique used to assay shear stress involves an orbital shaker. This method was first described by Dardik (Dardik et al, 2005) and Salek (Salek et al., 2011). This utilizes a medium- throughput system, exposing cells to fluid flow using commercially available culture plates placed on an orbital shaker (Warboys et al., 2014). This simple system has been used to determine the regulation of inflammation, permeability, senescence, proliferation, and apoptosis of ECs exposed to shear stress (Dardik et al, 2005; Kraiss et al., 2003; Warboys et al., 2010; Warboys et al., 2014).

Tensile stress- based studies include traditional 2D in vitro polyacrylamide models where substrate variation is amenable has demonstrated that cell spreading, migration and proliferation has consequentially increased with ECM matrix stiffness, depending on the tumor cell subpopulation and patient (Grundy et al 2016; Kim et al., 2014; Wong et al., 2015; Umesh et al., 2014; Pathak et al., 2012). While others have demonstrated cell spreading in 2D increases with elastic modulus (Thomas et al., 2000). Collagen matrix variation has suggested that matrix biophysical properties can influence phenotype (Diao et al., 2019; Fernandez-Fuente et al., 2014). Moreover, in the context of 2D, modulation hyaluronic acid (HA) hydrogel elastic modulus suggested that CD44, binding receptor for HA, is mechanosensitive; while elastic modulus affects microRNA expression in GBMs (Kim et al., 2014; Rape et al., 2015; Ananthanarayanan et al., 2011). Conversely, 3D in vitro physiologically relevant matrix models have utilized the use of polymer- hydrogel combinations such as HA- PEG (hyaluronic acid, polyethylene glycol) and

demonstrated that, similar to current 2D methods, matrix elastic modulus affects ECM deposition (Wang et al., 2014).

Typical methods to study the role compressive stress in the cell involve the two-dimensional (2D) nature of cell culture. This usually entails flat cell and nuclear morphologies that are not typical of in vivo contexts. Likewise, other traditional approaches to study compressive stress typically involve 2D systems where cells are confined through their apical surface and an opposing solid compressing surface such as poly(dimethylsiloxane) (PDMS) (He et al., 2018; Le Berre et al., 2014), or agarose (Aureille et al., 2019). Other methods such as glass surfaces (Caille et al., 2002; Petters et al., 2005), and 5μm beads on an atomic force microscopy (AFM) have been used to indent apical surfaces of cells (ofek et al., 2009) as means of applied compressive stress. However, 2D methods allow for mechanistic and controlled probing of cells in combination with potential of high resolutions imaging, which has uncovered key information of the cellular response to mechanical stress. By contrast, physiologically related in vitro protocols of compression consist of the use of compression to cell-containing three-dimensional (3D) matrix hydrogels (Boyle et al., 2020), the expansion of tumor spheroids in confining gels (Tse et al., 2012), and osmotically induced collapse of the ECM to compress tumor spheroids (Dolega et al., 2021). Much of the conventional methods surrounding the study and manipulation of compressive stress present limitations. This includes abnormally flat surfaces where cells are cultured on acquire nuclear and cell morphologies that are not physiologically representative of in vivo contexts. Despite advances toward more physiologically relevant approaches in 3D in vitro systems involving the addition of compressive stress on single cells embedded in 3D collagen hydrogels (Boyle et al., 2020), the confinement of cell aggregates on micropatterned shapes (Tse et al., 2012), and tumor aggregates subjected to high molecular weight dextran (Dolega et al., 2021) there remains a lack in mechanisms with which to isolate and manipulate compressive stresses in a controlled manner while attaining high resolution imaging capabilities simultaneously. Likewise, in vivo unidirectional cranial window-based compression methods onto

tumors fail to both capture the multidirectional behavioral response of compressive forces exerted by the tumor (Nia et al., 2020), and isolate one biophysical force from another. Altogether, of the described stresses discussed here: shear, tensile, and compressive, there is a deficiency in appropriate mechanisms to effectively study compressive stress in biological systems in a controlled 3D in vivo- like manner. These facts motivated us to design a tractable microfluidic culturing device that is amenable to manipulating compressive stresses on 3D tissues in a controlled manner, where GBMs will serve as our model system.

GLIOBLASTOMA MULTIFORME

Glioblastoma (GBM) is the most common and aggressive primary adult brain tumor with a median survival time of ~16 months (Stupp et al., 2009). The typical treatment for these tumors consists of surgical resection, followed by chemotherapy and radiotherapy (Stupp et al., 2009). However, GBMs demonstrate a diffuse invasive pattern, by which tumor cells either migrate individually or collectively infiltrate the surrounding healthy tissue away from the tumor margin (Watanabe et al., 1992), making complete surgical resection virtually impossible (Young et al., 2015). Current radiotherapy procedures cover a 2 cm margin beyond the visible tumor margin; however, microscopic tumor invasion may spread beyond this distance (Sherriff et al., 2013). Infiltrating tumor cells are enriched with glioblastoma stem cells, which are tumor cells which are distinguished by their ability to recapitulate the vast heterogeneity of GBM cell phenotypes through both propagation and differentiation (Eyler et al., 2008). It is this stem-like behavior in GBM cells that are often highly noncompliant to chemotherapy, driving tumor recurrence and chemoresistance (Franceschi et al., 2009; Barnes et al., NCB 2018). One step towards developing therapeutic opportunities in GBMs include targeting the cellular and noncellular components of the tumor microenvironment, which consists of ECM, interstitial fluid and various stromal cells (for instance, astrocytes, macrophages, and endothelial cells) (Quail et al.,2017). Considerable advances have already been made in understanding the microenvironmental

contributions to the progression of other cancers, particularly breast cancer (Levental et al., 2009; Nakasone et al., 2012; Ghajar et al., 2013; Provenzano et al., 2009) and pancreatic cancer (Laklai et al., Nat Med 2016; Elahi et al., 2019; Provenzano et al., 2012). Thus, new therapies have also been developed to target the GBM tumor microenvironment (De et al., 2017; Jain et al., 2014).

While growing in the confinement of the skull, GBMs in patients are known to produce increased intracranial pressures (10-100 mmHg) as compared with matched controls (0-5 mmHg) (Alberti et al., 1978). In GBM, cells within the tumor displace non-neoplastic astrocytes, which, along with vascular abnormalities, result in defective barrier properties within the brain, inducing vessel permeability that allows plasma and fluid to leak into the tumor tissue, which consequentially induces cerebral edema and increasing intracranial fluid pressure (IFP) (Heldin et al., 2004). These events then result in fluid accumulation that compresses the tumor and surrounding normal tissue and reduces cellular uptake in solid tumors (Heldin et al., 2004).

It is clear that the GBM microenvironment is mechanically challenged and thus impacting glioma behavior. In vivo, where GBMs naturally develop under compressive stresses, it's been shown that stiff GBM tumors with wild-type (WT) isocitrate dehydrogenase-1 IDH1, a metabolic enzyme whose mutation is associated with greater progression-free survival (Cancer Genome Atlas Research et al., 2015; Reitman et al., 2010), have necrotic cores and present with an atypical and compromised vasculature, resulting in oxygen tension and signaling event through hypoxia-inducible factor-1α (HIF1α), a transcription factor that acts as a leading effector of hypoxia. HIF1α directly binds to the promoter of glycoprotein tenascin-C (TNC) and induces its transcription (Reitman et al., 2010; Miroshnikova et al., 2016). In brief, TNC behaves as an ECM modifier by cross-linking lecticans, which are non-covalently bound to HA. This HA–lectican–TNC complex (a corrupted version of the perineuronal net (PNN) structure, which serves as a structural scaffold to maintain the integrity of adult neuronal wiring and control of plasticity) stiffens the tumor tissue relative to the non-malignant brain through limiting ECM flexibility (Mouw et al., 2014; Day et al., 2004; Kim and Kumar, 2014). Since elevated amounts of HA are produced in GBMs, tissue

stiffening is worsened in the disease state (Kim and Kumar, 2014). The capability of IDH1-mutant GBMs to sense hypoxia is blunted, and this results in significantly reduced production of HIF1α and TNC, thus impacting to the softer nature of IDH1-mutant GBMs (Miroshnikova et al., 2016). Remarkably, stiffening of the ECM can override this protective phenotype of blunted hypoxia signaling through the down regulation of the HIF1α-targeting microRNA miR-203 (Miroshnikova et al., 2016).

Investigations surrounding the mechanically challenged GBM microenvironment–tumor interactions are limited by a lack of model systems that precisely represent the human brain microenvironment. Biomaterials and microengineered devices offer the opportunity to recreate the brain- like mechanically challenged microenvironment, enabling mechanistic discovery and therapeutic screening in environments that mimic tissue more closely than conventional 2D culture paradigms. For instance, the traditional use of microwell compression assays (He et al., 2018; Le Berre et al., 2014) lack the design flexibility and fail to capture key compositional, structural and mechanical features. Moreover, even with current advances in micro engineered technologies to assay the behavioral consequences of solid stresses in both GBM and other biological systems (Boyle et al., 2020; Tse et al., 2012; Dolega et al., 2021; Nia et al., 2020), there remains a deficiency of tractable engineered integrated microsystems that can not only replicate the complex physiological functionality of 3D tissues, but the ability to precisely manipulate and isolate the dynamic and mechanically relevant stresses in the appropriate disease models is still needed. Here, we designed a novel microfluidic device that permits the precise manipulation of solid stresses on 3D tissue. Our microfluidic system allows for, but is not limited to, an integrated approach where modulation of ECM substrate and biomaterials, administration of 3D tissues, small molecule perturbations and culture medium is easily accessible. This new mechanism of manipulation of solid stresses in a 3D context has potential to offer a route towards precision medicine.

CHAPTER 2

INTRODUCTION

Mechanical properties of tumors and their associated stromal microenvironment contribute to the hallmarks of cancer (Nia et al., 2020; Northey et al., 2017). These aberrant mechanical properties include an increase in extracellular matrix deposition, remodeling and crosslinking that stiffen the stroma as well as microenvironment and impart solid stresses on the tumor cells. In particular, compressive solid stresses modulate the function of the cancerous cells and their associated stromal cells (Davies & Tripathis, 1993; Illkhanizadeh et al., 2018). Compressive stresses accumulate as solid tumors grow within a confined microenvironment and begin to displace the surrounding stiffened stroma (Jain, Martin, & Stylianopoulos, 2014).

Compressive solid stress in tumors can range from 0.7 to 75 mmHg (0.1–10 kPa) for human tumors and 2 to 60 mmHg (0.25–8 kPa) for murine tumors (Nia et al., 2016, 2020; Stylianopoulos, Munn, & Jain, 2018). Compressive solid stresses can also accumulate on cancer cells that migrate through narrow interstitial spaces of the tissue (Friedl & Alexander, 2011). Compressive solid stresses in tumors also impacts drug delivery and efficiency by compromising the tissue vasculature. For example, accumulated compressive solid stress in solid tumors can be high enough that blood vessels become constricted (Griffon-Etienne, Boucher, Brekken, Suit, & Jain, 1999; Padera et al., 2004; Stylianopoulos et al., 2012).

Typical methods to study the role compressive stress in the cell involve two- dimensional (2D) cell culture where cells are confined at the bottom of a microwell through their basal surface, from here, a solid surface such as poly(dimethylsiloxane) (PDMS) is used to apply compression to the apical regions of the cell (He et al., 2018; Le Berre et al., 2014), or agarose (Aureille et al., 2019). Other methods use glass surfaces (Caille et al., 2002; Petters et al., 2005), and atomic force microscopy (AFM) to indent apical surfaces of cells (ofek et al., 2009). By contrast, in vitro

assays of compression have utilized cell-containing three-dimensional (3D) matrix hydrogels (Boyle et al., 2020), the expansion of tumor spheroids in confining gels (Tse et al., 2012), and osmotically induced collapse of the ECM to compress tumor spheroids (Dolega et al., 2021). Much of the conventional methods surrounding the study and manipulation of compressive stress present limitations, such as abnormally flat surfaces where cells being cultured acquire nuclear and cell morphologies that are not physiologically representative of the in vivo tissue context.

Despite advances toward more physiologically relevant approaches in 3D in vitro culture models involving the addition of compressive stress on single cells embedded in 3D collagen hydrogels (Boyle et al., 2020), the confinement of cell aggregates on micropatterned shapes (Tse et al., 2012), and tumor aggregates subjected to fluidic compression driven by osmotic forces from high molecular weight dextran (Dolega et al., 2021) there remains a lack in mechanisms with which to isolate and manipulate compressive stresses in a controlled manner while attaining high resolution imaging capabilities simultaneously. Likewise, in vivo unidirectional cranial window-based compression methods onto tumors fail to both capture the multidirectional behavioral response of compressive forces exerted by the tumor (Nia et al., 2020), isolate one biophysical force from another, study molecular signals, and monitor cell behaviors in response specifically to compression. Altogether, there is a deficiency in appropriate mechanisms to effectively study compressive stress in biological systems in a controlled 3D in vivo- like manner. These facts motivated us to design a tractable microfluidic culturing device that is amenable to manipulating compressive stresses on 3D tissues in a controlled manner.

RESULTS

A biomimetic microfluidic device to manipulate compressive solid stresses on 3D tissues

The goal of this study was to design, fabricate, and validate a culturing system that permits controlled applications of compressive solid stress on 3D tissues. To meet these needs, we

designed a biomimetic microfluidic device with specific criteria. This microsystem needed to be amenable to high resolution live cell imaging, biochemical assays, easy access for administration of cellular content and cell medium. Additionally, this system needed to withstand 30% strain in our desired hyaluronic acid (HA) hydrogel, as 30% strain has been correlated with compressive solid stresses associated with tumors which grow in confinement (Illkhanizadeh et al., 2018). To accommodate these amenities and construct this microfluidic system, we utilize PDMS to fabricate the microfluidic device and permanently bind it to a glass coverslip. The geometric design of this microfluidic device consists of one continuous hollow outer microchamber (pressure chamber) that is separated by thin (72μm) PDMS walls that connect a single hollow microwell (Figure 1B). These hollow microchambers are fabricated via photolithography and soft lithography. As air is injected into the inlet to introduce compression, the PDMS walls undergo an inward elastic deformation to directly subject CSS onto the contents of the microwell. The entirety of this single layer microdevice is only 500μm in height and 23,000 μm in diameter, with both outer and inner chambers only micrometers in width (Figure 1B). In total, the compartmentalized configuration of these microchambers make this system fully amenable for high resolution imaging, manipulation of cell matrix mechanics, cell nutrients, and easy delivery of 3D tissues (Figure 1B- 1D). This microfluidic system reproduces key structural, functional, and biomechanical properties and provides the isolation of specific biophysical solid stresses and can clarify the caliber of impact on behavioral responses in 3D tissues.

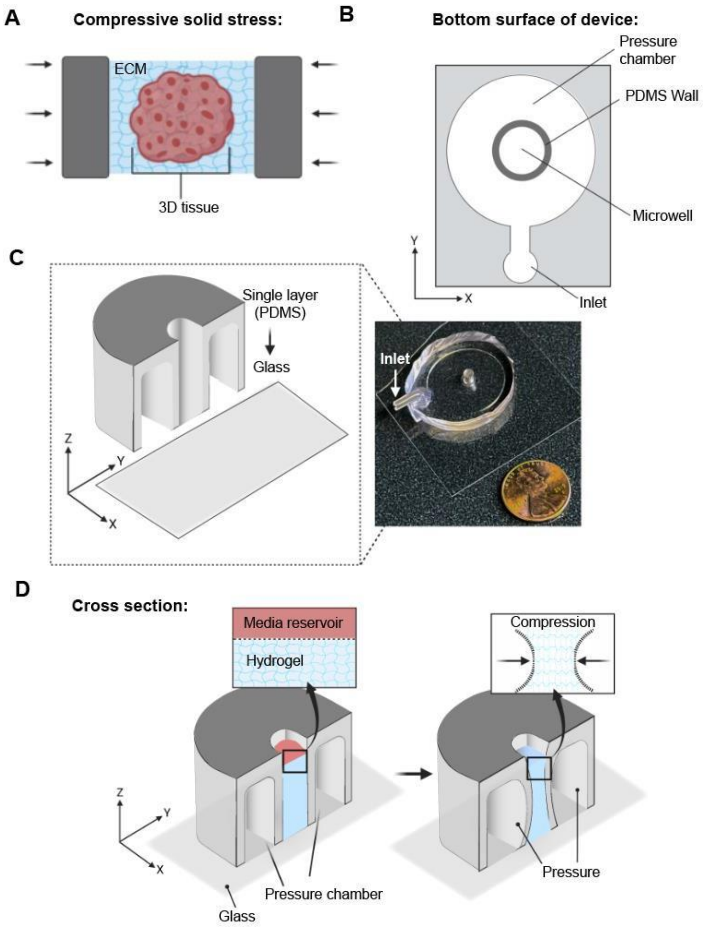

Figure 1.2: A new microfluidic culturing device to manipulate compressive solid stresses in 3D tissue.

(A) Schematic illustrating compressive solid stress onto 3D tissue.
(B) 2D illustration depicting the bottom surface of the microfluidic device.
(C) A 3D cross section cartoon demonstrating the device as a single PDMS that is permanently bound to glass. Adjacent to the cartoon is a real- life image of the microfluidic device. The penny demonstrates scaling.
(D) 3D cross section illustration of how this device works under compressive solid stress.

FEA reveals the final form factor of the biomimetic microfluidic device

To optimize the design of our microfluidic device we used FEA to manipulate key parameters of the device (SolidWorks: Dassault Systèmes), this includes: 1) height of the microwell, 2) width of the microwell, and 3) thickness of the PDMS wall. This microfluidic system is dependent on the

inward deformation of the PDMS walls when subjected to compression (Figure 1.1D). For these reasons the height and width of the microwell were modified in this study based on strain outputs predicted via FEA. The inputs to initiate our simulation experiments in FEA included the specific material properties of PDMS (1:10), and of our 2% solution of 30% methacrylated 65kDa HA hydrogel (gift of Dr. Jason Burdick) (Table 2.1:Supplementary Figure 2). Through these simulations we aimed to establish an output of 30% strain production in our HA hydrogel, as previously demonstrated (Illkhanizadeh et al., 2018), and examined whether entities of the microfluidic device such as the PDMS walls behaved as expected.

In the simulation phase of these studies, we found adjustments of key design parameters played a role in enabling the production of 30% strain in the HA hydrogel and deciding upon a final form factor of this microfluidic device. This included altering the heights and widths of the microwell, HA hydrogel, and the thickness of the PDMS walls. We found that initial design parameters that included a microwell- HA hydrogel height of 500μm, PDMS wall thickness of 50μm, and a HA- hydrogel width of 3,000μm with the application of 10kPa of compression produced ~300% strain (Table 1.3). From here, we increased both the width of the HA- hydrogel from 3,000μm to 4,000μm, and amount of compression from 10kPa to 16kpa, which resulted in ~250% strain. At this step, we enhanced the PDMS wall thickness from 50μm to 72μm, and increased compression from 16kpa to 22kPa, showed ~20% strain. Finally, simply increasing the amount of compression from 22kPa to 32kPa with these design parameters revealed 30% strain production in our microfluidic system, ultimately finalizing our design (Table 1.4). We show that with these specific design parameters we can elicit 30% strain within our system.

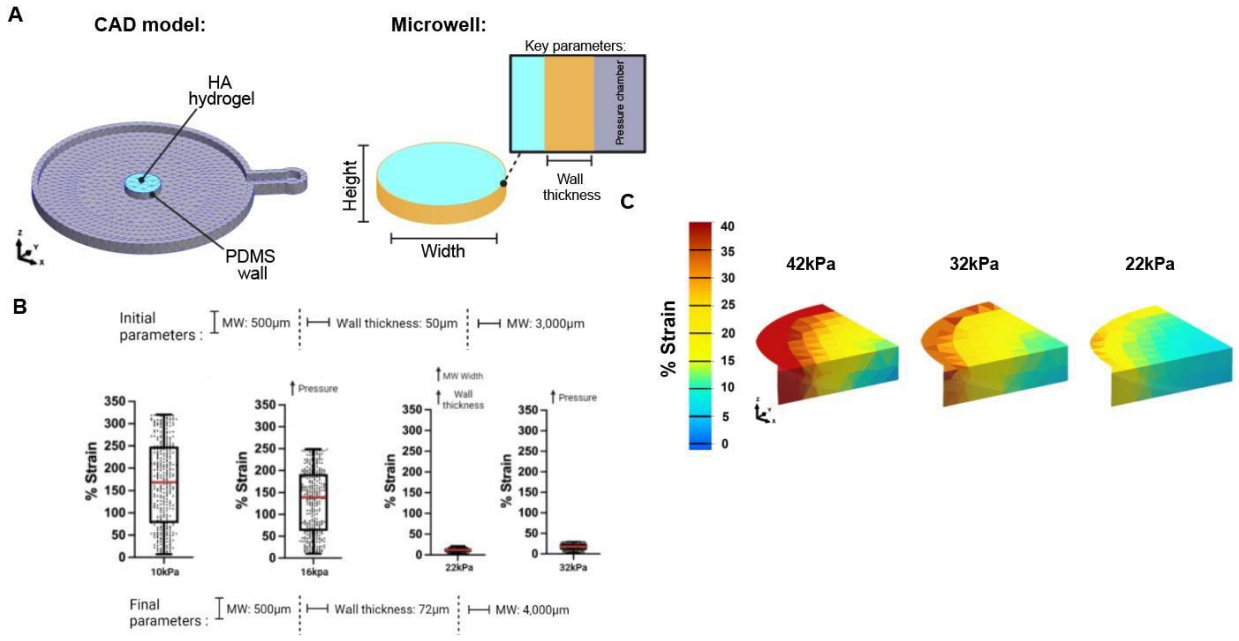

Figure 2.1: Finite element analysis reveals the final form factor.

(A) Illustration of CAD Model. Shows the overview of the model and its entities, to the right shows a cartoon of the microwell and key parameters altered in finite element analysis.
(B) Graphs demonstrating initial parameters and how modifications to key parameters have optimized the final form factor of this microfluidic device.
(C) Finite element analysis shows increase in the percent strain with increased pressure in the final form factor, with 32kPa accomplishing target strain of 30%. Abbreviations: MW: microwell, CAD: computer automated design.

3D vector fields demonstrate finite element analysis and experimental displacements align in the biomimetic microdevice

Next, we sought to validate our FEA predictions experimentally. We first performed rheology testing on our HA hydrogel and measured a stiffness of 1654Pa, which for our studies is relevant to the physiological GBM ECM (Barnes et al., 2017). From here, we tracked PDMS wall movement by embedding fluorescent beads into our HA- hydrogel, and with the application of 30% compression we found that the behavior of the PDMS walls in our microfluidic device precisely mimicked our finite element analysis (FEA) predictions. Moreover, through the application of this fluorescent bead experiment, we assayed several pressure variations and utilized particle image

velocimetry (PIV) algorithms (Barrasa-Fano et al., 2021) to measure strain via bead displacements. These experiments resulted in 3D vector fields suggesting displacements that were experimentally within proximity with the displacements predicted by FEA in our microfluidic device.

PDMS is gas permeable which could lead to a stress- relaxation response in our desired materials (PDMS and HA hydrogel). For these reasons we performed a pressure sustainability assay in our device. We implemented fluorescent beads within our HA- hydrogel, applied 30% strain, and used PIV as previously described (Barrasa-Fano et al., 2021), which resulted in a mean displacement of ~14μm in 14 hours. This assay permitted us to calculate the appropriate amount of air to re-inject into our system to sustain 30% strain in our experiments (Table 1.5).

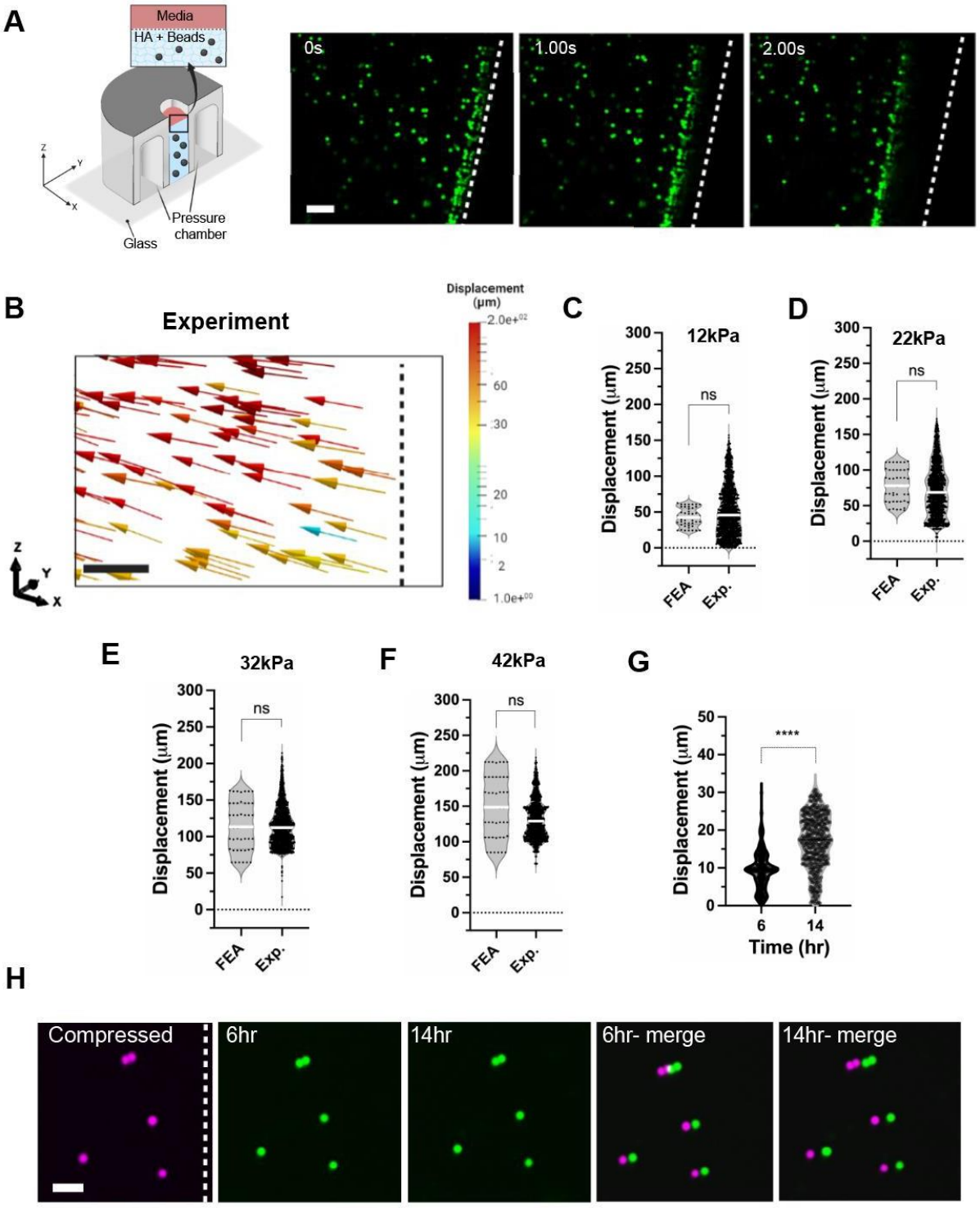

Figure 3.1: Experimental displacements validate finite element analysis predictions.

(A) Schematic (left) demonstrating the addition of florescent beads (4μm) in the HA- hydrogel. (right) time-lapse video of bead movement under compression of 30% strain. Scale bar: 50 μm. White dotted line depicts PDMS wall.

Figure 3.1 continued.
(B)3D vector field tracking bead displacement under compression of 30% strain using particle image velocimetry. Scale bar: 100μm. Black dotted line depicts PDMS wall.
(C- F) Quantification of displacement at various tested pressures. ****p < 0.05, n.s. = not significant.
(G) Quantification of bead displacements at 6 and 14 hours under sustained compression (30% strain).
(H) Confocal images of fluorescent beads at 6 and 14 hours under sustained compression (30% strain). Scale bar: 50μm. White dotted line depicts PDMS wall.

Patient- derived GBM neurospheres show increased area under compressive solid stress

After validating our microfluidic device, we sought to examine the behavioral response of compressive stress on 3D tissue. In these studies, we utilize GBMs as a model for compressive stress as GBMs, in patients, are well known to produce increased intracranial pressures (10-100 mmHg) as compared with matched controls (0-5 mmHg) (Alberti et al., 1978), suggesting their growth under compression.

Patient- derived GBM5 neurospheres were grown on 1% agarose for 4 days. To control for neurosphere size, we selected for spheroids between 5μm -105μm by filtering them through a membrane containing 105μm pore sizes. Since spheroid sizes of 500 μm has been associated with a necrotic core (Wolf et al., 2019), we opted to select for smaller neurospheres. From here, GBM5 neurospheres were implemented into the HA- hydrogel and into microfluidic device where were subjected to either no compression or with compression at 0% or 30% strain, respectively, for 48 hours (Figure 4.1). Furthermore, the appropriate amounts of air to reinject to sustain 30% strain was calculated as described above. Interestingly, we find that added compression of 30% strain is sufficient to induce increases in area of patient- derived GBM neurospheres, when compared to matched controls (Figure 4), and that this response of increased area under compressive stress might involve the phosphorylation of focal adhesion kinase (pFAK) (Figure 4), which is demonstrated to increase with malignancy in GBM in vivo (Barnes et al., 2018).

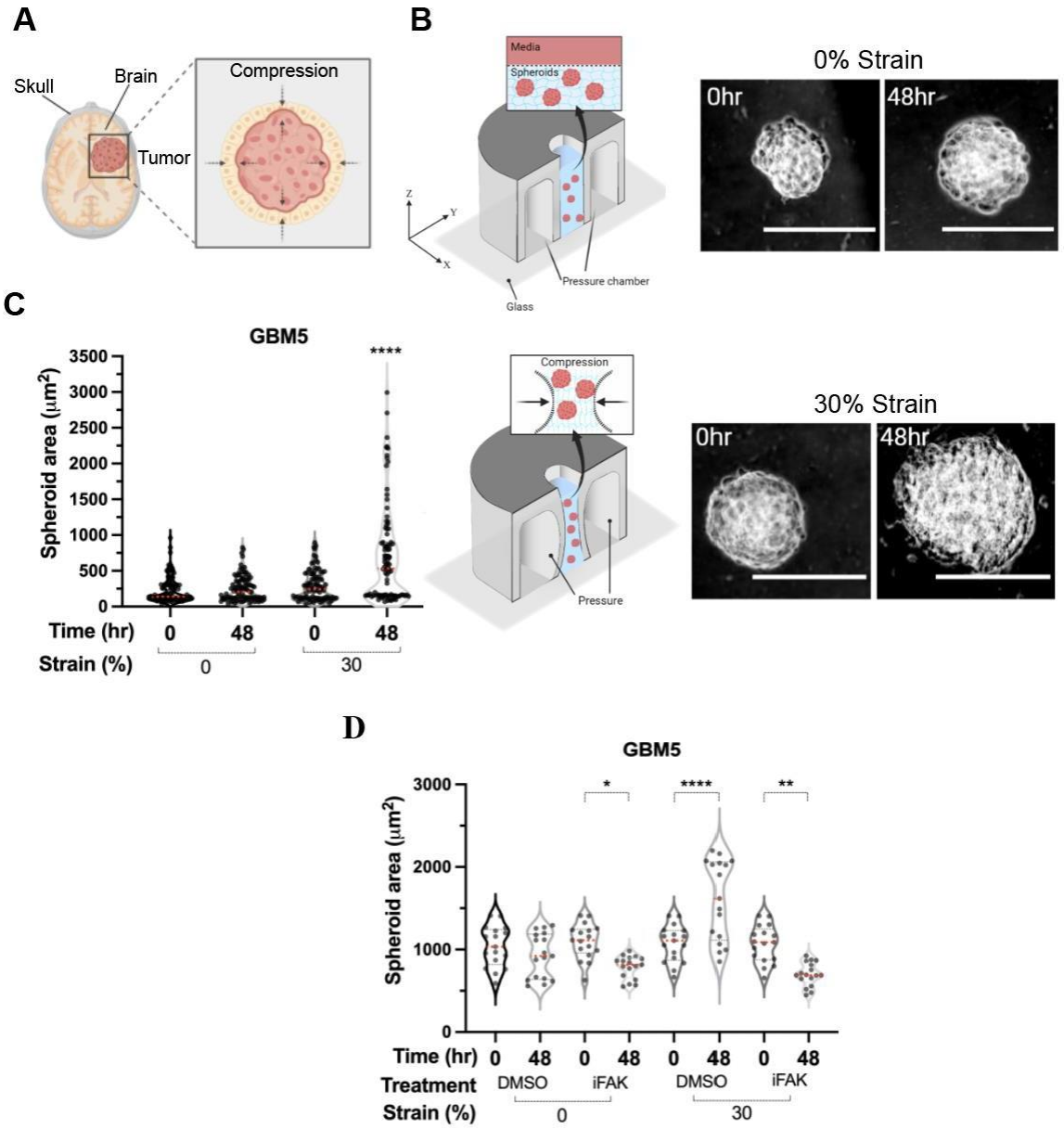

Figure 4.1: Compression of 30% strain yields an increase in GBM neurosphere area.
(A) Overview of tumor growth in confinement and illustrating compression.
(B) (left) cartoon showing the experimental setup (right) brightfield images (10X) of GBM5
(C) neurospheres under no compression and 30% compression at 0 and 48 hours. Scale bar: 100μm. Images displayed as inverted.
(D) Quantification of neurosphere area under 0% and 30% compression over 0 and 48 hours.
(E) Quantification of neurosphere area under 0% and 30% compression over 0 and 48 hours and treated with 5μM focal adhesion kinase inhibitor.
****p < 0.05, **p < 0.01, *p < 0.001.

DISCUSSION

Here we described the design, engineering, and calibration and application of a tractable microfluidic culturing device that can manipulate solid stresses in a controlled manner. We show that production of 30% strain in our system was coupled with specific design parameters within our system. We describe how the dimensions of the microwell, and especially of the PDMS walls played an important role in the decision of the final form factor of the microfluidic device. Rheology testing of our HA- hydrogel revealed a stiffness of 1,654Pa, that precisely mimics ECM stiffness reported in GBM (Barnes et al., 2017: Barnes et al., 2018). Additionally, we validated this microfluidic system and show that our experimental displacements align with predictions made by FEA. Further, we show that compression at 30% strain is sustainable. More importantly we accomplish the task of isolating compressive solid stress with our system and are able to execute strain manipulations precisely. Interestingly, we reveal that 30% strain induces increases in area of patient- derived GBM neurospheres, and this response of increased size to solid stress might involve the phosphorylation of focal adhesion kinase (pFAK), which is demonstrated to increase with malignancy in GBM (Barnes et al., 2018). In vivo, confined tumors such as GBMs are extensively described as being associated with high contractility and integrin activity, a common molecular signature of mechanosignaling in GBMs (Barnes et al., 2018; Barnes et al., 2017; Miroshnikova et al., 2016). Unlike in vivo approaches our microfluidic system allows for the isolation of compressive stresses where mechanistic approaches can be used to elucidate the molecular signals that are especially associated with the behavioral responses in these confined tumor models.

Future applications

This microfluidic device could be operated as a co-culturing mechanism to elucidate the role of mechanics (solid stress) on immune or vascular endothelial cells in the context of brain

tumors. Moreover, acute traumatic brain injury could be modeled with slight modifications. This includes the incorporation of tumorspheres with the addition of cyclic compression (as opposed to static), allowing for high- speed, reversible compressive stress to be applied).

This tractable microfluidic system can be used to apply other solid stresses including tension. In addition, this system can model other diseases that include (but not limited to) solid masses as well such as breast, pancreas, head, and neck- related carcinomas. Our system is fully amenable of incorporating all cell types and disease models to better understand the role of solid stresses on behavior. Furthermore, this microfluidic culturing system allows for complete modulation of ECM material, which could elucidate the role of stiff vs compliant matrices in addition to solid stresses in a specific disease model. In addition, since the microwell of this device is easily accessible, one could learn how growth factors secreted under the respective solid stresses might contribute to specific behavioral responses via media collection. Finally, due to the simplicity of our microfluidic culturing platform, drug- screening for agents that can protect against the adverse effects of mechanical forces in various disease models can be accomplished.

Advantages

This microengineered microfluidic device enables unprecedented investigation of the casual effects of brain tumor- generated solid stresses on the surrounding physiologically relevant and functional ECM, coupled with the dynamic, isolated, and controlled manipulation of solid stresses. One of the advantages of my microfluidic system is that it supports longitudinal intravital microscopy during the compression stages. Another key advantage is the ability to precisely control the magnitude and rate of mechanical displacement under solid stress applications. Laboratories that have access to photolithography and soft lithography- based materials to create this microfluidic device will be able to easily implement and adapt this system for different

applications. The caliber of solid stress and ECM/ 3D hydrogel can be easily tailored to the disease model of interest.

Another key advantage is the potential to use this tool in combination with other assays. For instance, alongside intravital high resolution imaging, our system is amenable for performing immunofluorescence enabling mechanistic experiments. Moreover, it is usually possible to perform only short-term experiments (i.e., on the order of days), however my microfluidic device allows for both short- and long- term experiments. Another advantage to this device is owed to the inexpensive costs of the polymer (PDMS) it is constructed from, this device is capable of being upscaled (easily casted from silicone master molds acquiring the microfluidic pattern) to support high- throughput experiments.

LIMITATIONS OF THE STUDY

The main potential limitation of using our microfluidic device is the requirement for relatively advanced expertise in photolithography and soft lithography methods. We recommend surveying the literature for microfabrication protocols commonly employed for generating microfluidic devices. Additionally, a potential limitation to this microfluidic device involves the performance of immunofluorescence when using the ECM/3D hydrogel of interest. For these reasons we recommend performing rheological- based testing to determine the material properties and pore sizes of the desired ECM/ 3D hydrogel. Those data could inform the success of preferred immunofluorescence protocols. To circumvent potential issues surrounding immunofluorescence in a chosen hydrogel pore size involves the utilization of obtaining snap- frozen sections. Moreover, another limiting feature to this system involves the collection of protein for immunoblotting- based experiments. To address these concerns, we recommend upscaling the number of devices used per experiment, this will optimize the amount of protein extracted. In total,

we have developed a tractable microdevice that can employ controlled mechanistic approaches to elucidate the role of solid stresses in 3D tissues.

Beyond the study of compressive solid stresses on primary patient- derived brain tumors, this tractable microfluidic device could also be utilized in other preclinical models of diseases with solid masses in the brain, such as ‘tumor-like’ infectious lesions (cysts or abscesses); benign masses (e.g., those resulting from abnormal neurogenesis, neurofibromatosis types I and II, tuberous sclerosis, and von Hippel–Lindau syndrome); tumefactive multiple sclerosis plaques; and extreme vascular malformations (Huisman et al., 2009; Cunliffe et al., 2009).

Table 1.1: List of key reagents and resources used in this study

REAGENT OR RESOURCES	SOURCE	IDENTIFIER
Chemicals, peptides, and instruments		**cat. no.**
Sylgard 184 silcone elastomer base	Dow	02065622
Sylgard 184 silicone base elastomer curing agent	Dow	02065622
SU-8- 2150	Kayakli	19100850
Silicone wafer 76.2 ±0.63mm		SK0731
Trichloro (1H, 1H, 2H, 2H- perfluoroctyl) silane	Sigma	78560-45-9
O.C.T compound	Tissue- Tek	4416-00
ClearWeld quick setting epoxy	JB Weld	R1232A-H1205A-1239B
Sucrose		
Equipment		**Model**
Spin coater		HL-650MZ- 23NPPB0
Harrick Plasma- Plasma cleaner		PDC- 001
Vacuum Gauge		PDC- VCG
Programmable syringe pump		NE-4000

Table 1.2: List of finite element analysis inputs.

SOLIDWORKS: Finite element analysis inputs		
PDMS material properties	**Value**	**Units**
Elastic modulus	2.66	MPa
Poison's ratio	0.49	------
Shear modulus	0.82	MPa
Mass density	1030	kg/m^3
Tensile strength	6.7	MPa
Compressive strength	2.7	MPa
Yield strength	0.7	MPa
Thermal conduction	0.27	W (m · k)
Hyaluronic acid	**Value**	**Units**
Elastic modulus	1,654	Pa
Poison's ratio	0.48	------
Shear modulus	$7.5e^{-05}$	MPa
Finite element analysis mesh details		**Value**
Mesh size		0.5mm
Element size		0.059mm
Tolerance		0.029mm
Total nodes		19,894
Maximum aspect ratio		53.86

Table 1.3: Initial finite element analysis parameters.

Pressure (kPa)	Width of pressure chamber (μm)					
	18,400					
	PDMS wall width (μm)					
	50					
	Height (μm)					
	400		500		600	
	Width of microwell (μm)					
	3,000	4,000	3,000	4,000	3,000	4,000
	% Strain range					
25	14- 400	17- 480	16- 390	14- 530	25- 750	25- 850
24	13- 390	16- 450	14- 370	13- 510	22- 680	20- 800
22	12- 360	15- 420	13- 340	12- 460	19- 580	2- 750
20	10- 320	13- 380	12- 310	11- 420	19- 580	18- 700
18	10- 320	13- 380	12- 310	11- 420	19- 580	18- 700
16	9- 260	11- 320	10- 250	8- 340	15- 440	15- 550
14	9- 230	9- 280	9- 220	8- 300	13- 390	13-490
12	6- 200	9- 230	8- 190	8- 300	11- 350	13- 420
10	4- 160	9- 200	6- 150	7- 320	10- 290	12- 350
8	2- 130	9- 160	6- 140	4- 170	8- 250	11- 280
6	1- 970	8- 120	6-120	4- 130	5- 170	8- 200
4	6- 64	8- 85	6- 62	3- 83	4- 42	6- 65
2	3- 32	4- 42	3- 31	2- 41	2- 21	3- 33
1.5	2- 24	3- 32	2- 23	1- 31	2- 16	2- 24

Table 1.4: Final finite element analysis parameters.

Pressure (kPa)	Height of microwell (μm)
	500
	Width of microwell (μm)
	4,000
	Width of pressure chamber in mm
	24,660
	PDMS wall width (μm)
	72
	% Strain range
42	4- 39
38	4- 35
32	3- 30
27	3- 25
22	2- 21
17	2- 16
12	1- 11
7	1- 7

Table 1.5: Air required for strain under various pressures and their respective displacements.

Pressure (kPa)	Air required (μL)	% Strain	Displacement (μm)
42	85.28	4- 39	21.2- 212
38	77.16	4- 35	19.1- 192
32	65.17	3- 30	16.1- 162
27	54.83	3- 25	13.6- 137
22	44.67	2- 21	11.1- 111
17	34.52	2- 16	8.5- 86
12	24.37	1- 11	6.1- 61
7	14.21	1- 7	3.5- 35

CHAPTER 3

Discussion and conclusions

APPLICATIONS

In chapter 2, I described the design, engineering, and calibration and application of a tractable microfluidic culturing device that can manipulate solid stresses in a controlled manner. I showed that using specific design parameters I was able to elicit 30% compression (strain) within our system. Specifically, 30% strain was produced within my HA hydrogel (desired ECM). Additionally, the behavior of the PDMS walls in my device precisely mimicked our finite element analysis (FEA) predictions. Moreover, through particle image velocimetry (PIV) algorithms I was able to measure strain via bead displacements and found that our microfluidic device demonstrated displacements that experimentally validated displacements predicted by FEA. PDMS is known to be gas permeable which could potentiate a stress- relaxation response in our materials (PDMS and HA hydrogel). For these reasons I performed a pressure sustainability assay in our device which resulted in a mean displacement of ~14μm in 14 hours. This assay enabled me to calculate the appropriate amount of air to re-inject into our system to sustain 30% compression in my experiments. Further, I also demonstrate that 30% compression is sufficient to induce the expansion of patient- derived GBM neurospheres, and this response of increased size to solid stress might involve the phosphorylation of focal adhesion kinase (pFAK), which is demonstrated to increase with malignancy in GBM (Barnes et al., 2018).

Beyond the study of compressive solid stresses on primary patient- derived brain tumors, this tractable microfluidic device could also be utilized in other preclinical models of diseases with solid masses in the brain, such as ‘tumor-like’ infectious lesions (cysts or abscesses); benign masses (e.g., those resulting from abnormal neurogenesis, neurofibromatosis types I and II,

tuberous sclerosis, and von Hippel–Lindau syndrome); tumefactive multiple sclerosis plaques; and extreme vascular malformations (Huisman et al., 2009; Cunliffe et al., 2009).

Additionally, this microfluidic device could be utilized as a co-culturing mechanism to elucidate the role of mechanics (solid stress) on immune or vascular endothelial cells in the context of brain tumors. Moreover, acute traumatic brain injury could be modeled with slight modifications. This includes the incorporation of tumorspheres with the addition of cyclic compression (as opposed to static), allowing for high- speed, reversible compressive stress to be applied).

This tractable microfluidic system can be used to apply other solid stresses including tension. In addition, this system can model other diseases that include (but not limited to) solid masses as well such as breast, pancreas, head, and neck- related carcinomas. My system is fully amenable of incorporating all cell types and disease models to better understand the role of solid stresses on behavior. Furthermore, this microfluidic culturing system allows for complete modulation of ECM material, which could elucidate the role of stiff vs compliant matrices in addition to solid stresses in a specific disease model. In addition, since the microwell of this device is easily accessible, one could learn how growth factors secreted under the respective solid stresses might contribute to specific behavioral responses via media collection. Finally, due to the simplicity of our microfluidic culturing platform, drug- screening for agents that can protect against the adverse effects of mechanical forces in various disease models can be accomplished.

ADVANTAGES AND LIMITATIONS

This microengineered microfluidic device enables unprecedented investigation of the casual effects of brain tumor- generated solid stresses on the surrounding physiologically relevant and functional ECM, coupled with the dynamic, isolated, and controlled manipulation of solid stresses. One of the advantages of my microfluidic system is that it supports longitudinal intravital microscopy during the compression stages. Another key advantage is the ability to precisely

control the magnitude and rate of mechanical displacement under solid stress applications. Laboratories that have access to photolithography and soft lithography- based materials to create this microfluidic device will be able to easily implement and adapt this system for different applications. The caliber of solid stress and ECM/ 3D hydrogel can be easily tailored to the disease model of interest.

Another key advantage is the potential to use this tool in combination with other assays. For instance, alongside intravital high resolution imaging, our system is amenable for performing immunofluorescence enabling mechanistic experiments. Moreover, it is usually possible to perform only short-term experiments (i.e., on the order of days), however my microfluidic device allows for both short- and long- term experiments. Another advantage to this device is owed to the inexpensive costs of the polymer (PDMS) it is constructed from, this device is capable of being upscaled (easily casted from silicone master molds acquiring the microfluidic pattern) to support high- throughput experiments.

The main potential limitation of using my device is the requirement for relatively advanced expertise in photolithography and soft lithography methods. I recommend surveying the literature for microfabrication protocols commonly employed for generating microfluidic devices. Additionally, a potential limitation to this microfluidic device involves the performance of immunofluorescence when using the ECM/3D hydrogel of interest. For these reasons I recommend performing rheological- based testing to determine the material properties and pore sizes of the desired ECM/ 3D hydrogel. Those data could inform the success of preferred immunofluorescence protocols. To circumvent potential issues surrounding immunofluorescence in a chosen hydrogel pore size involves the utilization of obtaining snap- frozen sections. Moreover, another limiting feature to this system involves the collection of protein for immunoblotting- based experiments. To address these concerns, I recommend upscaling the number of devices used per experiment, this will optimize the amount of protein extracted. In total,

I have developed a tractable microdevice that can employ controlled mechanistic approaches to elucidate the role of solid stresses in 3D tissues.

REFERENCES

Ananthanarayanan, B., Kim, Y. & Kumar, S. Elucidating the mechanobiology of malignant brain tumors using a brain matrix–mimetic hyaluronic acid hydrogel platform. Biomater.32, 7913–7923 (2011).

Aureille, J., Buffière-Ribot, V., Harvey, B. E., Boyault, C., Pernet, L., Andersen, T., … Guilluy, C. (2019). Nuclear envelope deformation controls cell cycle progression in response to mechanical force. EMBO reports, 20(9), e48084. https://doi.org/10.15252/embr.201948084

Ayad NME, Kaushik S, Weaver VM. Tissue mechanics, an important regulator of development and disease. Philosophical Transactions of the Royal Society B: Biological Sciences. 2019;374(1779):20180215.

Barrasa-Fano J, Shapeti A, Jorge-Peñas Á, Barzegari M, Sanz-Herrera JA, Van Oosterwyck H. TFMLAB: A MATLAB toolbox for 4D traction force microscopy. *SoftwareX*. 2021;15:100723.

Barnes JM, Przybyla L, Weaver VM. Tissue mechanics regulate brain development, homeostasis and disease. Ewald A, ed. Journal of Cell Science. 2017;130(1):71-82.

Barnes JM, Kaushik S, Bainer RO, et al. A tension-mediated glycocalyx–integrin feedback loop promotes mesenchymal-like glioblastoma. Nat Cell Biol. 2018;20(10):1203-1214.

Bataller, R., and Brenner, D.A. (2005). Liver fibrosis. J. Clin. Invest.115,209–218.

Blewett, C.J., Zgleszewski, S.E., Chinoy, M.R., Krummel, T.M., and Cilley, R.E.(1996). Bronchial ligation enhances murine fetal lung development in whole-or-gan culture. J. Pediatr. Surg.31, 869–877.

Bowden N, Bryan MT, Duckles H, et al. Experimental approaches to study endothelial responses to shear stress. Antioxidants & Redox Signaling. 2016;25(7):389-400.

Buschmann MH, Dieterich P, Adams NA, and Schnittler H-J. Analysis of flow in a cone-and-plate apparatus with respect to spatial and temporal effects on endothelial cells. Biotech Bioeng 89: 493–502, 2005.

Budday S, Nay R, de Rooij R, Steinmann P, Wyrobek T, Ovaert TC, Kuhl E. 2015. Mechanical properties of gray and white matter brain tissue by indentation. J. Mech. Behav. Biomed. Mater. 46, 318–330. (10.1016/j.jmbbm.2015.02.024)

Chatelin S, Constantinesco A, Willinger R. 2010. Fifty years of brain tissue mechanical testing: from in vitro to in vivo investigations. Biorheology 47, 255–276. (10.3233/BIR-2010-0576)

Chaudhuri, O., Cooper-White, J., Janmey, P.A. *et al.* Effects of extracellular matrix viscoelasticity on cellular behaviour. *Nature* **584,** 535–546 (2020).

Cheng JPX, et al. 2015. Caveolae protect endothelial cells from membrane rupture during increased cardiac output. J. Cell Biol. 211, 53–61. (10.1083/jcb.201504042)

Chiu JJ. Wang DL. Chien S. Skalak R. Usami S. Effects of disturbed flow on endothelial cells. J Biomech Eng. 1998;120:2–8.

Cunliffe, C. H. et al. Intracranial lesions mimicking neoplasms. *Arch. Pathol. Lab. Med.* **133**, 101–123 (2009).

Dai G, Kaazempur-Mofrad MR, Natarajan S, Zhang Y, Vaughn S, Blackman BR, Kamm RD,

Dardik A, Chen L, Frattini J, Asada H, Aziz F, Kudo FA, and Sumpio BE. Differential effects of orbital and laminar shear stress on endothelial cells. **Soc Vasc Surg** 41: 869–880, 2005.

De Vleeschouwer, S. & Bergers, G. in GlioblastomaCh. 16 (ed De Vleeschouwer, S.) (Codon Publications, 2017).

Davies PF, Dewey CF, Bussolari SR, Gordon EJ, and Gimbrone MA. Influence of hemodynamic forces on vascular endothelial function. In vitro studies of shear stress and pinocytosis in bovine aortic cells. **J Clin Invest** 73: 1121–1129, 1984.

Day J. M., Olin A. I., Murdoch A. D., Canfield A., Sasaki T., Timpl R., Hardingham T. E. and Aspberg A. (2004). Alternative splicing in the Aggrecan G3 domain influences binding interactions with tenascin-C and other extracellular matrix proteins. *J. Biol. Chem.* 279, 12511-12518. 10.1074/jbc.M400242200

Diao, W. et al. Behaviors of glioblastoma cells in in vitro microenvironments. Sci. Rep.9, 85 (2019).

Dintwa E, Tijskens E, Ramon H. 2008. On the accuracy of the Hertz model to describe the normal contact of soft elastic spheres. Granul. Matter. 10, 209–221. (10.1007/s10035-007-0078-7)

Dragovich MA, Chester D, Fu BM, Wu C, Xu Y, Goligorsky MS, Zhang XF. 2016. Mechanotransduction of the endothelial glycocalyx mediates nitric oxide production through activation of TRP channels. Am. J. Physiol.-Cell Physiol. 311, C846–C853. (10.1152/ajpcell.00288.2015)

Elahi-Gedwillo, K. Y., Carlson, M., Zettervall, J. & Provenzano, P. P. Antifibrotic therapy disrupts stromal barriers and modulates the immune landscape in pancreatic ductal adenocarcinoma. Cancer Res.79, 372–386 (2019).

Eyler, C. E. & Rich, J. N. Survival of the fittest: cancer stem cells in therapeutic resistance and angiogenesis. J. Clin. Oncol.26, 2839–2845 (2008).

Franceschi, E. et al. Treatment options for recurrent glioblastoma: pitfalls and future trends. Expert Rev. Anticancer. Ther.9, 613–619 (2009).

Fernandez-Fuente, G., Mollinedo, P., Grande, L., Vazquez-Barquero, A. & Fernandez-Luna, J.

L. Culture dimensionality influences the resistance of glioblastoma stem-like cells to multi-kinase inhibitors. Mol. Cancer Ther.13, 1664–1672 (2014).

Garcia-Cardena G, and Gimbrone MAJr. Distinct endothelial phenotypes evoked by arterial waveforms derived from atherosclerosis-susceptible and -resistant regions of human vasculature. **Proc Natl Acad Sci U S A** 101: 14871–14876, 2004

Greaves GN, Greer AL, Lakes RS, Rouxel T. Poisson's ratio and modern materials. Nature Mater. 2011;10(11):823-837.

Galford E, McElhaney H. 1970. A viscoelastic study of scalp, brain and dura. J. Biomech. 3, 211–221. (10.1016/0021-9290(70)90007-2)

Ghajar, C. M. et al. The perivascular niche regulates breast tumour dormancy. Nat. Cell Biol.15, 807–817 (2013).

Grundy, T. J. et al. Differential response of patient-derived primary glioblastoma cells to environmental stiffness. Sci. Rep.6, 23353 (2016).

Gudi S, Nolan JP, and Frangos JA. Modulation of GTPase activity of G proteins by fluid shear stress and phospholipid composition. **Proc Natl Acad Sci U S A** 95: 2515–2519, 1998.

Guz N, Dokukin M, Kalaparthi V, Sokolov I. 2014. If cell mechanics can be described by elastic modulus: study of different models and probes used in indentation experiments. Biophys. J. 107, 564–575. (10.1016/j.bpj.2014.06.033)

Harding, R., Hooper, S.B., and Han, V.K. (1993). Abolition of fetal breathing movements by spinal cord transection leads to reductions in fetal lung liquid volume, lung growth, and IGF-II gene expression. Pediatr. Res.34, 148–153.

Huisman, T. A. Tumor-like lesions of the brain. *Cancer Imaging* **9**(Special Issue A), S10–S13 (2009).

Jain, A. et al. Guiding intracortical brain tumour cells to an extracortical cytotoxic hydrogel using aligned polymeric nanofibres. Nat. Mater.13, 308–316 (2014).

Kim, Y. & Kumar, S. CD44-mediated adhesion to hyaluronic acid contributes to mechanosensing and invasive motility. Mol. Cancer Res.12, 1416–1429 (2014).

Kraiss LW, Alto NM, Dixon DA, McIntyre TM, Weyrich AS, and Zimmerman GA. Fluid flow regulates E-selectin protein levels in human endothelial cells by inhibiting translation. **J Vasc Surg** 37: 161–168, 2003.

Kruse SA, Rose GH, Glaser KJ, Manduca A, Felmlee JP, Jack CR, Ehman RL. 2008. Magnetic resonance elastography of the brain. Neuroimage 39, 231–237. (10.1016/j.neuroimage.2007.08.030)

Kwon MY, Wang C, Galarraga JH, Puré E, Han L, Burdick JA. Influence of hyaluronic acid modification on CD44 binding towards the design of hydrogel biomaterials. Biomaterials. 2019;222:119451.

Lee S, Kassianidou E, Kumar S. 2018. Actomyosin stress fiber subtypes have unique viscoelastic properties and roles in tension generation. Mol. Biol. Cell. 29, 1992–2004. (10.1091/mbc.E18-02-0106)

Lo HP, et al. 2015. The caveolin–cavin system plays a conserved and critical role in mechanoprotection of skeletal muscle. J. Cell Biol. 210, 833–849. (10.1083/jcb.201501046)

Levental, K. R. et al. Matrix crosslinking forces tumor progression by enhancing integrin signaling. Cell139, 891–906 (2009).

Lin K. Hsu PP. Chen BP. Yuan S. Usami S. Shyy JY. Li YS. Chien S. Molecular mechanism of endothelial growth arrest by laminar shear stress. Proc Natl Acad Sci U S A. 2000;97:9385–9389.

Lu Y-B, et al.. 2006. Viscoelastic properties of individual glial cells and neurons in the CNS. Proc. Natl Acad. Sci. USA 103, 17 759–17 764. (10.1073/pnas.0606150103)

Nagel T, Resnick N, Atkinson WJ, Dewey CF, and Gimbrone MA. Shear stress selectively upregulates intercellular adhesion molecule-1 expression in cultured human vascular endothelial cells. **J Clin Invest** 94: 885–891, 1994.

Neglia, J.P., Fitzsimmons, S.C., Maisonneuve, P., Scho ni, M.H., Scho ni-Affolter, F., Corey, M., and Lowenfels, A.B. (1995). The risk of cancer amongpatients with cystic fibrosis. Cystic fibrosis and cancer Study Group.N. Engl. J. Med.332, 494–499.

Nelson, C.M., Gleghorn, J.P., Pang, M.F., Jaslove, J.M., Goodwin, K., Varner,V.D., Miller, E., Radisky, D.C., and Stone, H.A. (2017). Microfluidic chest cav-ities reveal that transmural pressure controls the rate of lung development.Development144, 4328–4335.

Nixon SJ, Carter A, Wegner J, Ferguson C, Floetenmeyer M, Riches J, Key B, Westerfield M, Parton RG. 2007. Caveolin-1 is required for lateral line neuromast and notochord development. J. Cell Sci. 120, 2151–2161. (10.1242/jcs.003830)

Miroshnikova Y. A., Mouw J. K., Barnes J. M., Pickup M. W., Lakins J. N., Kim Y., Lobo K., Persson A. I., Reis G. F., Mcknight T. R. et al. (2016). Tissue mechanics promote IDH1-dependent Hif1alpha-tenascin C feedback to regulate glioblastoma aggression. *Nat. Cell Biol*. [Epud ahead of print] doi:10.1038/ncb3429. 10.1038/ncb3429.

Mouw J. K., Ou G. and Weaver V. M. (2014). Extracellular matrix assembly: a multiscale deconstruction. *Nat. Rev. Mol. Cell Biol.* 15, 771-785. 10.1038/nrm3902

Nakasone, E. S. et al. Imaging tumor–stroma interactions during chemotherapy reveals contributions of the microenvironment to resistance. Cancer Cell21, 488–503 (2012).

Natural and Synthetic Biomedical Polymers. Chapter 4. Elsevier; 2014

Nigro P, Abe J ichi, Berk BC. Flow shear stress and atherosclerosis: a matter of site specificity. Antioxidants & Redox Signaling. 2011;15(5):1405-1414.

Nawaz S, Sánchez P, Bodensiek K, Li S, Simons M, Schaap IAT. 2012. Cell visco-elasticity measured with AFM and optical trapping at sub-micrometer deformations. PLoS ONE 7, e45297 (10.1371/journal.pone.0045297)

Northcott JM, Dean IS, Mouw JK, Weaver VM. Feeling stress: the mechanics of cancer progression and aggression. Front Cell Dev Biol. 2018;6:17.

Pathak, A. & Kumar, S. Independent regulation of tumor cell migration by matrix stiffness and confinement. Proc. Natl. Acad. Sci. USA109, 10334–10339 (2012).

Pogoda K, et al.. 2014. Compression stiffening of brain and its effect on mechanosensing by glioma cells. New J. Phys. 16, 075002 (10.1088/1367-2630/16/7/075002)

Provenzano, P. P., Inman, D. R., Eliceiri, K. W. & Keely, P. J. Matrix density-induced mechanoregulation of breast cell phenotype, signaling and gene expression through a FAK–ERK linkage. Oncogene28, 4326–4343 (2009).

Provenzano, P. P. et al. Enzymatic targeting of the stroma ablates physical barriers to treatment of pancreatic ductal adenocarcinoma. Cancer Cell21, 418–429 (2012).

Quail, D. F. & Joyce, J. A. The microenvironmental landscape of brain tumors. Cancer Cell31, 326–341 (2017).

Rape, A. D., Zibinsky, M., Murthy, N. & Kumar, S. A synthetic hydrogel for the high-throughput study of cell–ECM interactions. Nat. Commun.6, 8129 (2015).

Reitman Z. J., Olby N. J., Mariani C. L., Thomas R., Breen M., Bigner D. D., McLendon R. E. and Yan H. (2010). IDH1 and IDH2 hotspot mutations are not found in canine glioma. *Int. J. Cancer* 127, 245-246. 10.1002/ijc.25017.

Rico F, Roca-Cusachs P, Gavara N, Farré R, Rotger M, Navajas D. 2005. Probing mechanical properties of living cells by atomic force microscopy with blunted pyramidal cantilever tips. Phys. Rev. E 72, 021914 (10.1103/PhysRevE.72.021914)

Sack I, Beierbach B, Hamhaber U, Klatt D, Braun J. 2008. Non-invasive measurement of brain viscoelasticity using magnetic resonance elastography. NMR Biomed. 21, 265–271. (10.1002/nbm.1189)

Salek MM, Sattari P, and Martinuzzi RJ. Analysis of fluid flow and wall shear stress patterns inside partially filled agitated culture well plates. **Ann Biomed Eng** 40: 707–728, 2011.

Sherriff, J. et al. Patterns of relapse in glioblastoma multiforme following concomitant chemoradiotherapy with temozolomide. Br. J. Radiol.86, 20120414 (2013).

Stupp, R. et al. Effects of radiotherapy with concomitant and adjuvant temozolomide versus radiotherapy alone on survival in glioblastoma in a randomised phase III study: 5-year analysis of the EORTC-NCIC trial. Lancet Oncol.10, 459–466 (2009).

Thomas, T. W. & DiMilla, P. A. Spreading and motility of human glioblastoma cells on sheets of silicone rubber depend on substratum compliance. Med. Biol. Eng. Comput.38, 360–370 (2000).

Ueba H, Kawakami M, and Yaginuma T. Shear stress as an inhibitor of vascular smooth muscle cell proliferation—role of transforming growth factor-beta 1 and tissue-type plasminogen activator. **Arterioscler Thromb Vasc Biol** 17: 1512–1516, 1997.

Umesh, V., Rape, A. D., Ulrich, T. A. & Kumar, S. Microenvironmental stiffness enhances glioma cell proliferation by stimulating epidermal growth factor receptor signaling. PLoS One9, e101771 (2014).

Wagner CT, Durante W, Christodoulides N, Hellums JD, and Schafer AI. Hemodynamic forces induce the expression of heme oxygenase in cultured vascular smooth muscle cells. **J Clin Invest** 100: 589–596, 1997.

Wang, C., Tong, X. & Yang, F. Bioengineered 3D brain tumor model to elucidate the effects of matrix stiffness on glioblastoma cell behavior using PEG-based hydrogels. Mol. Pharm.11, 2115–2125 (2014).

Warboys CM, Berson R, Mann GE, Pearson JD, and Weinberg PD. Acute and chronic exposure to shear stress have opposite effects on endothelial permeability to macromolecules. **Am J Physiol-Heart Circ Physiol** 298: H1850–H1856, 2010.

Warboys CM, de Luca A, Amini N, Luong L, Duckles H, Hsiao S, White A, Biswas S, Khamis R, Chong CK, Cheung W-M, Sherwin SJ, Bennett MR, Gil J, Mason JC, Haskard DO, and Evans PC. Disturbed flow promotes endothelial senescence via a p53-dependent pathway. **Arterioscler Thromb Vasc Biol** 34: 985–995, 2014.

Watanabe, M., Tanaka, R. & Takeda, N. Magnetic resonance imaging and histopathology of cerebral gliomas. Neuroradiology34, 463–469 (1992).

Wolf, K.J., Chen, J., Coombes, J.D. *et al.* Dissecting and rebuilding the glioblastoma microenvironment with engineered materials. *Nat Rev Mater* **4**, 651–668 (2019). https://doi.org/10.1038/s41578-019-0135-y

Wong, S. Y. et al. Constitutive activation of myosin-dependent contractility sensitizes glioma tumor-initiating cells to mechanical inputs and reduces tissue invasion. Cancer Res.75, 1113–1122 (2015).

Yin W, Shanmugavelayudam SK, and Rubenstein DA. The effect of physiologically relevant dynamic shear stress on platelet and endothelial cell activation. **Thromb Res** 127: 235–241, 2011.

Young, R. M., Jamshidi, A., Davis, G. & Sherman, J. H. Current trends in the surgical management and treatment of adult glioblastoma. Ann. Transl. Med.3, 121 (2015).

Publishing Agreement

It is the policy of the University to encourage open access and broad distribution of all theses, dissertations, and manuscripts. The Graduate Division will facilitate the distribution of UCSF theses, dissertations, and manuscripts to the UCSF Library for open access and distribution. UCSF will make such theses, dissertations, and manuscripts accessible to the public and will take reasonable steps to preserve these works in perpetuity.

I hereby grant the non-exclusive, perpetual right to The Regents of the University of California to reproduce, publicly display, distribute, preserve, and publish copies of my thesis, dissertation, or manuscript in any form or media, now existing or later derived, including access online for teaching, research, and public service purposes.

DocuSigned by:
Gretchen Ford
54A71B646B89413...
Author Signature

10/21/2022
Date